

## Fine structure in the $\alpha$ decay of $^{156}\text{Lu}$ and $^{158}\text{Ta}$

E. Parr,<sup>1,\*</sup> R. D. Page,<sup>1</sup> D. T. Joss,<sup>1</sup> F. A. Ali<sup>†‡</sup>,<sup>1</sup> K. Auranen<sup>§</sup>,<sup>2</sup> L. Capponi<sup>¶</sup>,<sup>3,4</sup> T. Grahn,<sup>2</sup> P. T. Greenlees,<sup>2</sup> J. Henderson<sup>\*\*</sup>,<sup>5</sup> A. Herzán,<sup>6,2</sup> U. Jakobsson,<sup>2</sup> R. Julin,<sup>2</sup> S. Juutinen,<sup>2</sup> J. Konki<sup>††</sup>,<sup>2</sup> M. Labiche,<sup>7</sup> M. Leino,<sup>2</sup> P. J. R. Mason,<sup>7</sup> C. McPeake,<sup>1</sup> D. O'Donnell<sup>‡‡</sup>,<sup>1</sup> J. Pakarinen,<sup>2</sup> P. Papadakis,<sup>1</sup> J. Partanen,<sup>2</sup> P. Peura,<sup>2</sup> P. Rahkila,<sup>2</sup> J. P. Reville,<sup>1</sup> P. Ruotsalainen,<sup>2</sup> M. Sandzelius,<sup>2</sup> J. Sarén,<sup>2</sup> C. Scholey,<sup>2</sup> J. Simpson,<sup>7</sup> J. F. Smith,<sup>3,4</sup> M. Smolen,<sup>3,4</sup> J. Sorri<sup>§§</sup>,<sup>2</sup> S. Stolze<sup>¶¶</sup>,<sup>2</sup> A. Thornthwaite,<sup>1</sup> and J. Uusitalo<sup>2</sup>

<sup>1</sup>Oliver Lodge Laboratory, University of Liverpool, Liverpool, L69 7ZE, United Kingdom

<sup>2</sup>University of Jyväskylä, Department of Physics, P.O. Box 35, FI-40014 Jyväskylä, Finland

<sup>3</sup>School of Engineering and Computing, University of the West of Scotland, Paisley, PA1 2BE, United Kingdom

<sup>4</sup>SUPA, Scottish Universities Physics Alliance, Glasgow G12 8QQ, UK

<sup>5</sup>Department of Physics, University of York, Heslington, York, YO10 5DD, United Kingdom

<sup>6</sup>Institute of Physics, Slovak Academy of Sciences, SK-84511 Bratislava, Slovakia

<sup>7</sup>Nuclear Physics Group, STFC Daresbury Laboratory, Daresbury, Warrington WA4 4AD, United Kingdom

(Dated: April 2, 2019)

Fine structure in the  $\alpha$  decay of high-spin states in  $^{156}\text{Lu}$  and  $^{158}\text{Ta}$  has been identified by means of  $\alpha\gamma$ -coincidence analysis. One new  $\alpha$  decay from  $^{156}\text{Lu}$  and two from  $^{158}\text{Ta}$  were identified, one of which was found to populate a previously unknown state in  $^{154}\text{Lu}$ . The hindrance-factor systematics from all four odd-odd,  $N = 85$  nuclei with known  $\alpha$ -decaying,  $\pi h_{11/2}$  coupled states were reviewed and are discussed. These proved consistent with the previously assigned  $(\pi h_{11/2} \nu h_{9/2})10^+$  configuration of the  $\alpha$ -decaying state in  $^{156}\text{Lu}$ ; which differs from the  $(\pi h_{11/2} \nu f_{7/2})9^+$  assignments in the other three nuclei.

PACS numbers: 23.60.+e, 27.70.+q, 29.30.Ep, 29.30.Kv

Dr Edward Parr

### Address:

Oliver Lodge Laboratory,  
University Liverpool,  
Liverpool,  
L69 7ZE,  
UK

**Email:** [ep@ns.ph.liv.ac.uk](mailto:ep@ns.ph.liv.ac.uk)

### CORRESPONDING AUTHOR:

<sup>†</sup>Permanent address: Department of Physics, College of Education, University of Sulaimani, P.O. Box 334, Sulaimani, Kurdistan Region, Iraq.

<sup>‡</sup>Present address: Department of Physics, University of Guelph, Guelph, Ontario N1G 2W1, Canada.

<sup>§</sup>Present address: Physics Division, Argonne National Laboratory, Argonne, Illinois 60439, USA.

<sup>¶</sup>Present address: ELINP, Horia Hulubei National Institute for Research in Physics and Nuclear Engineering, Bucharest-Măgurele, Romania.

<sup>\*\*</sup>Present address: Lawrence Livermore National Laboratory, 7000 East Avenue, Livermore, CA 94550, USA.

<sup>††</sup>Present address: CERN, CH-1211 Geneva 23, Switzerland

<sup>‡‡</sup>Present address: School of Engineering and Computing, University of the West of Scotland, Paisley, PA1 2BE, United Kingdom.

<sup>§§</sup>Present address: Sodankylä Geophysical Observatory, University of Oulu, Sodankylä, Finland.

<sup>¶¶</sup>Present address: Physics Division, Argonne National Laboratory, Argonne, Illinois 60439, USA.

\*Electronic address: [ep@ns.ph.liv.ac.uk](mailto:ep@ns.ph.liv.ac.uk)

## I. INTRODUCTION

Excited states of the proton-rich nuclei around  $N = 82$  are most commonly interpreted in terms of single-particle configurations. This is due to the semi-doubly-magic nucleus of  ${}^{146}_{64}\text{Gd}_{82}$  which gives shell, and semi-shell, closures at  $N = 82$  and  $Z = 64$  respectively [1–3]. Although much work has been carried out to study nuclear states in this region, there remains very little known of the  $\alpha$ -decay fine structure from and to these states. Experimental results of  $\alpha$ -decay fine structure can be instructive when assigning different nucleonic configurations for both the initial and final states. For example the reduced hindrance factors of  $\alpha$  decays provide a measure for the similarity of the initial and final nuclear states populated in the decay process. Additionally,  $\alpha$  decay can populate levels which may not be accessible when using other experimental techniques and level schemes previously constructed may also be confirmed. The lack of experimental  $\alpha$ -decay fine-structure information in this region is partly due to the high energy of the single-particle excited states in many of the nuclei. As the partial half-life of an  $\alpha$  decay is strongly dependent on its  $Q$  value, the branching ratios of  $\alpha$  decays to these excited states can be very small in comparison to those which populate ground states. One potentially fruitful area of study, however, is the fine structure in the  $\alpha$  decays between odd-odd nuclei. In these systems the coupling of the odd proton and neutron provide low-energy excited states, where no pair breaking or excitations into higher-energy nucleon orbitals are required. The  $\alpha$  decays to these states are therefore not inhibited by a large reduction in  $\alpha$ -decay  $Q$  value.

This paper reports on the study of the fine structure in the  $\alpha$  decay of the odd-odd  $N = 85$  isotones  ${}^{156}\text{Lu}$  and  ${}^{158}\text{Ta}$ , populating states in  ${}^{152}\text{Tm}$  and  ${}^{154}\text{Lu}$ , respectively. The low-energy states in odd-odd nuclei above  ${}^{146}\text{Gd}$  tend to couple an odd  $\nu f_{7/2}$ ,  $\nu h_{9/2}$  or  $\nu i_{13/2}$  neutron to either a  $\pi s_{1/2}$ ,  $\pi d_{3/2}$  or  $\pi h_{11/2}$  proton. Due to the large spin changes required, internal transitions between states where the odd proton populates the  $\pi h_{11/2}$  orbital to those in which either the  $\pi s_{1/2}$  or  $\pi d_{3/2}$  orbitals are populated are rare. This generally leads to two states in the odd- $Z$  nuclei of the region where  $\alpha$  or proton decay dominates; these corresponding to the lowest-energy states with an odd proton in either the  $\pi h_{11/2}$  orbital or the  $\pi s_{1/2}$ ,  $\pi d_{3/2}$  orbitals [4]. It is the states in which the odd proton occupies the  $\pi h_{11/2}$  orbital in  ${}^{156}\text{Lu}$  and  ${}^{158}\text{Ta}$ , as well as in the daughter nuclei  ${}^{152}\text{Tm}$  and  ${}^{154}\text{Lu}$ , that have been studied. They will be referred to as high-spin states in this paper with the lowest in energy of these being considered the ground state. Two new  $\alpha$  decays from  ${}^{158}\text{Ta}$  and one from  ${}^{156}\text{Lu}$  have been identified and the wider systematics of  $\alpha$ -decay hindrance factors from high-spin states in odd-odd,  $N = 85$  nuclei are discussed in terms of the structures of both the decaying and populated states.

## II. PREVIOUS STUDIES

### A. High-spin, $\alpha$ -decaying states in odd-odd, $N = 85$ isotones

High-spin,  $\alpha$ -decaying states in four  $N = 85$ , odd-odd isotones have been reported. These were identified in  ${}^{152}\text{Ho}$  [ $E_\alpha = 4453(3)$  keV,  $T_{1/2} = 52.3(5)$  s] [5–7],  ${}^{154}\text{Tm}$  [ $E_\alpha = 5031(3)$  keV,  $T_{1/2} = 2.98(20)$  s] [8, 9],  ${}^{156}\text{Lu}$  [ $E_\alpha = 5565(4)$  keV,  $T_{1/2} = 198(2)$  ms] [10–12], and  ${}^{158}\text{Ta}$  [ $E_\alpha = 6046(4)$  keV,  $T_{1/2} = 35(1)$  ms] [11–13]. A  $J^\pi = 19^-$ ,  $\alpha$ -decaying, spin-trap isomer in  ${}^{158}\text{Ta}$  is also known [14], but will not be discussed in this paper. Fine structure in the  $\alpha$  decay of the states in  ${}^{152}\text{Ho}$  and  ${}^{154}\text{Tm}$ , to two excited states in  ${}^{148}\text{Tb}$  [15, 16] and one in  ${}^{150}\text{Ho}$  [9], respectively, have also previously been identified following  $\alpha\gamma$ -coincidence analysis.

The assignment of spins to these  $\alpha$ -decaying states was facilitated by  $\beta$ -decay branches from these levels. Studies of the branching ratios to different states in the daughter nuclei from the  $\beta$  decays of  ${}^{152}\text{Ho}$  [17], and  ${}^{154}\text{Tm}$  [9] allowed the decaying states to be assigned as having high-spin configurations. The high-spin assignment of the  $\alpha$ -decaying state in  ${}^{158}\text{Ta}$  was proposed in Ref. [13] following a study of the  $\alpha$ -decay chains, and proton emissions, starting with  ${}^{166}\text{Ir}$ .

The two lowest-lying high-spin states in these  $N = 85$  nuclei are expected to have  $(\pi h_{11/2}\nu f_{7/2})9^+$  and  $(\pi h_{11/2}\nu h_{9/2})10^+$  configurations. By using  $\gamma$ -ray spectroscopy, level schemes were constructed above the  $\alpha$ -decaying states in each of the nuclei to determine their configurations [18–21]. The spins and parities of the levels were assigned with the aid of the transitions' multipolarities, which were determined from conversion-electron intensities [18, 19],  $\gamma$ -ray intensity-balance arguments [18, 20, 21], and Weisskopf estimate considerations [18, 20, 21]. The states in  ${}^{152}\text{Ho}$  [18],  ${}^{154}\text{Tm}$  [19], and  ${}^{158}\text{Ta}$  [20] were assigned with  $(\pi h_{11/2}\nu f_{7/2})9^+$  configurations. However, the recently reported  $\gamma$ -ray study of  ${}^{156}\text{Lu}$  assigned the  $\alpha$ -decaying state with a  $(\pi h_{11/2}\nu h_{9/2})10^+$  configuration [21], lying 62 keV below the  $(\pi h_{11/2}\nu f_{7/2})9^+$  state.

### B. High-spin states in odd-odd, $N = 83$ nuclei populated following $\alpha$ decay

Detailed level schemes of high-spin states in all four of the  $N = 83$  daughter nuclei of the  $\alpha$ -decays discussed are known. These were constructed from spectroscopy of  $\gamma$  rays emitted promptly following the production by fusion evaporation of  ${}^{148}\text{Tb}$  [22, 23] and following internal isomeric decays in  ${}^{150}\text{Ho}$  [24, 25],  ${}^{152}\text{Tm}$  [25], and  ${}^{154}\text{Lu}$  [26, 27]. All four of the schemes were built on a  $(\pi h_{11/2}\nu f_{7/2})9^+$  ground state. Bands based on the  $[(\pi h_{11/2})^n\nu f_{7/2}]$  multiplet were also assigned above these ground states in  ${}^{150}\text{Ho}$  ( $n = 3$ ),  ${}^{152}\text{Tm}$  ( $n = 5$ ), and  ${}^{154}\text{Lu}$

( $n = 7$ ) with  $J^\pi = 11^+$ ,  $13^+$ , and  $15^+$  levels, terminating at a  $J^\pi = 17^+$  seniority isomer. It is assumed that each of the four  $\alpha$  decays discussed previously populate the lowest  $9^+$  ground states.

Additionally, states assigned with an  $(\pi h_{11/2} \nu f_{7/2}) 8^+$  configuration were identified in each of the nuclei. These low-energy states occur 316 keV ( $^{148}\text{Tb}$ ), 217 keV ( $^{150}\text{Ho}$ ), 115 keV ( $^{152}\text{Tm}$ ), and 22 keV ( $^{154}\text{Lu}$ ) above the ground states and their level energies were well reproduced by shell-model calculations [25].

The  $\alpha$  decay of  $^{152}\text{Ho}$  reported in Refs. [15, 16] populated high-spin states in  $^{148}\text{Tb}$  at 238 and 316 keV. These were assigned as the  $7^+$  and known  $8^+$  states of the  $(\pi h_{11/2} \nu f_{7/2})$  multiplet, respectively. Also, the  $\alpha$  decay of  $^{154}\text{Tm}$  was reported to populate a 197 keV state in  $^{150}\text{Ho}$  [9]. The configurational assignment of this state was not proposed in the reference.

### III. EXPERIMENTAL DETAILS

The data used to obtain the results presented were from an experiment performed at the Accelerator Laboratory of the University of Jyväskylä, Finland. The  $^{156}\text{Lu}$  and  $^{158}\text{Ta}$  nuclei were produced by a fusion-evaporation reaction using a  $^{58}\text{Ni}$  beam incident on a  $^{106}\text{Cd}$  target for 292 hours. The  $^{58}\text{Ni}$  beam had energy of 318 MeV with an average intensity of 6.4 particle nA. The target was a self-supporting  $^{106}\text{Cd}$  foil of thickness  $0.975 \text{ mg cm}^{-2}$ . The fusion-evaporation products were separated from other reaction products and unreacted beam ions using the RITU gas-filled recoil separator [28, 29]. They were then implanted into two double-sided silicon-strip detectors (DSSDs), which are part of the GREAT spectrometer [30], located at a focal plane of RITU. The two DSSDs each consisted of 40 horizontal and 60 vertical strips giving a total of 4800 individual pixels. An array of 28 silicon PIN diode detectors was located upstream from the DSSDs to detect charged particles emitted out of the DSSDs. To measure  $\gamma$  and X rays emitted by decaying implanted nuclei at the focal plane two detector systems were installed. A planar double-sided germanium strip detector located downstream of the DSSDs within the vacuum chamber of GREAT was used to measure predominantly low-energy  $\gamma$  and X rays. An array of three HPGe clover detectors was also placed around the DSSDs and designed to measure higher-energy  $\gamma$  rays at the focal plane. At the entrance of GREAT was a multi-wire proportional counter (MWPC). This measured the energy loss of incoming recoils which, along with the time-of-flight from the MWPC to the DSSDs, enabled the selection of desired recoils over incoming unreacted beam or other reaction products. The data analysis was performed using the GRAIN software [31], which was developed for use with data acquired by the Total Data Readout system [32].

### IV. DATA ANALYSIS

For the energy calibration of the DSSDs the  $\alpha$  particles emitted by recoiling nuclei produced during the experiment, or those in a subsequent decay chain, were utilised. Energies of  $\alpha$  particles from  $^{150}\text{Dy}$  [ $E_\alpha = 4233(4) \text{ keV}$ ] [7],  $^{152}\text{Er}$  [ $E_\alpha = 4799(3) \text{ keV}$ ] [7],  $^{157}\text{Hf}$  [ $E_\alpha = 5731(3) \text{ keV}$ ] [33],  $^{155}\text{Lu}$  [ $E_\alpha = 7390(5) \text{ keV}$ ] [12],  $^{156}\text{Hf}$  [ $E_\alpha = 7782(4) \text{ keV}$ ] [12], and  $^{158}\text{W}$  [ $E_\alpha = 8286(7) \text{ keV}$ ] [34] were used. To identify  $\alpha$  decays with small branching ratios populating excited states the technique of measuring coincident  $\alpha$  particles and  $\gamma$  rays was used. In the present results the  $\gamma$  rays were measured using the planar germanium detector. The absolute efficiency for the detection of  $\gamma$  rays in the planar germanium detector was determined using GEANT4 Monte Carlo simulations.

Candidates for  $\alpha$  decays from fusion-evaporation products were identified as signals in the DSSDs which did not have a coincident MWPC signal. As the recoiling nuclei were implanted close to the surface of the DSSDs a significant proportion ( $\sim 40\%$ ) of the  $\alpha$  particles were emitted out of the detectors, therefore depositing only a fraction of their energy. Some of these *escaping*  $\alpha$  particles were then also detected in the PIN detectors. The background signals in the DSSDs produced by the partial energy deposition of the escaping  $\alpha$  particles could, therefore, be reduced to some extent by vetoing  $\alpha$  particles when a coincident PIN signal was measured. Possible  $\alpha$  decays were also correlated with a preceding recoil implantation into the same pixel of the DSSD. The time between the recoil and  $\alpha$  decay was required to be less than 576 ms to identify decays from high-spin states in  $^{156}\text{Lu}$  [ $T_{1/2} = 198(2) \text{ ms}$ ] and 105 ms for those from  $^{158}\text{Ta}$  [ $T_{1/2} = 35(1) \text{ ms}$ ].

### V. RESULTS

The results from the study of the fine structure in the  $\alpha$  decay of high-spin isomers in  $^{156}\text{Lu}$  and  $^{158}\text{Ta}$  are given in Table I. The information given is: the  $\alpha$ -particle energies; the proposed spins, parities and energies of the final states populated; the total  $Q$  value of the decay,  $Q_T$ , which is the  $\alpha$ -decay  $Q$  value (which assumes the presently assigned masses of the  $\alpha$  emitters) plus the energy of the coincident  $\gamma$  ray; the branching ratios of the  $\alpha$  decays; and the reduced decay widths and hindrance factors, as described in Sec. VI. The proposed level schemes populated in  $^{152}\text{Tm}$  and  $^{154}\text{Lu}$  following the  $\alpha$  decay of the high-spin states in  $^{156}\text{Lu}$  and  $^{158}\text{Ta}$  are given in Fig. 1. The individual branching ratios were calculated using the total  $\alpha$ -decay branching ratios of  $b_\alpha = 98(9)\%$  ( $^{156}\text{Lu}$ ) and  $b_\alpha = 99(13)\%$  ( $^{158}\text{Ta}$ ) [12].

### A. $^{156}\text{Lu}(10^+) \rightarrow ^{152}\text{Tm}$ $\alpha$ -decay fine structure

Figure 2(a) shows the DSSD spectrum gated for the  $\alpha$  decays of  $^{156}\text{Lu}$ ; as described in Sec. IV. Panel (b) then shows the same spectrum with the additional requirement of a coincident 115-keV  $\gamma$  ray being measured in the planar germanium focal-plane detector. A background has been subtracted from this spectrum due to the random coincidences between high-intensity neighbouring  $\alpha$  particles, shown in Panel (a), and a continuum of  $\gamma$ -ray energies over 115 keV. Finally, Panel (c) shows the  $\gamma$ -ray spectrum measured in the planar germanium detector in coincidence with 5446-keV  $^{156}\text{Lu}$   $\alpha$  particles. A background has also been subtraction from this spectrum, mainly due to the high intensity of K X rays from various elements produced being measured in random coincidence with 5561-keV,  $^{156}\text{Lu}$   $\alpha$ -particles in the lower energy tail of the distribution.

The 5561-keV  $\alpha$  particles measured in 2(a) are assumed to be those previously measured from the high-spin state in  $^{156}\text{Lu}$  to the  $^{152}\text{Tm}$  ground state [10–12]. This is based on the consistency of the  $\alpha$ -particle energy with those previously reported and that it is not observed in coincidence with any  $\gamma$  rays. The  $\alpha$  particles with  $E_\alpha = 5446$  keV observed in coincidence with 115-keV  $\gamma$  rays have a  $Q_T$  value of 5704(6) keV. As this is consistent with the  $Q_T$  of the  $\alpha$  decay which directly populates the  $^{152}\text{Tm}(9^+)$  ground state, 5707(4) keV, it may be assumed that the  $\alpha$  decay directly populates a 115-keV energy level. As a state has previously been reported at 114.4(1) keV above the ground state with  $J^\pi = 8^+$  [25] we propose that this is the state populated by the  $\alpha$  decay.

As  $\alpha\gamma$  coincidence analysis was used to identify the new  $\alpha$ -decay, the branching ratio was calculated using the intensity corrected for internal conversion of the electromagnetic decay in the daughter nucleus. The K-shell conversion coefficient for the 115-keV transition in  $^{152}\text{Tm}$  was measured to be  $\alpha_K = 1.29(6)$  using the relative intensities of the K X rays and 115-keV  $\gamma$  rays in Fig. 2(c). By using the methods prescribed in Ref. [35] the total conversion coefficient,  $\alpha_{tot}$ , was found by varying the mixing ratio,  $\delta$ , between  $E2$  and  $M1$  transitions to achieve this  $\alpha_K$  value. This corresponds to a mixing ratio of  $\delta = 0.92$  and a total conversion coefficient of  $\alpha_{tot} = 1.96(3)$ . This value is in agreement with that previously measured of  $\alpha_{tot} = 2.1(3)$  in Ref. [25].

### B. $^{158}\text{Ta}(9^+) \rightarrow ^{154}\text{Lu}$ $\alpha$ -decay fine structure

Figure 3(a) shows the  $\alpha$ -particle energies measured in the DSSDs with the requirements applied for a  $^{158}\text{Ta}$  decay; as described in Sec. IV. Panels b(i) and b(ii) show the same  $\alpha$ -particle energies with the additional requirement of a coincident  $\gamma$  ray with  $E_\gamma = 22$  or 60 keV, respectively, being measured in the planar germanium detector at the focal plane. Finally, Panels c(i) and c(ii)

show the  $\gamma$  rays measured in the planar germanium detector which are in coincidence with  $\alpha$  particles with energies of 6021 and 5981 keV, respectively, measured in the DSSDs.

The  $\alpha$  particles measured with 6041 keV are taken to be those previously assigned to directly populate the  $^{154}\text{Lu}(9^+)$  ground state from the  $^{158}\text{Ta}$  high-spin state [11–13]. This may be assumed due to the consistency of the  $\alpha$ -particle energy with those previously measured and that it is not observed in coincidence with any  $\gamma$  rays. It is proposed that the (6021-keV  $\alpha$ -particle)-(22-keV  $\gamma$ -ray) coincidences in panels b(i) and c(i) are associated with the  $\alpha$  decays from  $^{158}\text{Ta}$  which populate a  $J^\pi = 8^+$  state in  $^{154}\text{Lu}$  which has previously been identified 22 keV above the  $9^+$  ground state [26, 27]. This assignment is made from the comparison of the total decay  $Q$  value of this  $\alpha$  decay,  $Q_T = 6200(4)$  keV, with that of the  $\alpha$  decay to the  $J^\pi = 9^+$  state,  $Q_T = 6198(4)$  keV. Finally, the  $\alpha\gamma$  coincidences in the panels b(ii) and c(ii) have  $Q_T = 6197(4)$  keV, which is consistent with the other two  $\alpha$  decays. Although no state has previously been identified 60 keV above the  $^{154}\text{Lu}$  ground state it is proposed that these coincidences represent an  $\alpha$  decay to a new state at that energy.

$M1$  multiplicities were assumed for the 22- and 60-keV transitions in  $^{154}\text{Lu}$  as the  $\gamma$  rays were measured in prompt coincidence with the  $\alpha$  decays. When considering the Weisskopf estimates for the transitions, corrected for internal conversions, only  $E1$  and  $M1$  multiplicities are compatible with prompt  $\gamma$  rays. As no parity change would be expected between low-energy  $\pi h_{11/2}$  states in  $^{154}\text{Lu}$  then  $M1$  multiplicities were assumed. This is consistent with the previous  $8^+$  assignment of the 22-keV level [26, 27] and also gives possible spin and parity assignments of  $J^\pi = 8^+, 9^+, \text{ or } 10^+$  for the 60-keV state. The total conversion coefficients used for the 22- and 60-keV transitions in  $^{154}\text{Lu}$  to calculate the  $\alpha$ -decay branching ratios were  $\alpha_{tot} = 52.2$  and 2.7, respectively. These were calculated using the method prescribed in Ref. [35] assuming the  $M1$  multiplicities.

## VI. DISCUSSION: $\alpha$ -DECAY HINDRANCE FACTORS

Table I gives the hindrance factors, HF, for each of the  $\alpha$  decays observed. These are derived from the reduced decay widths,  $\delta^2$ , which were calculated using the method prescribed by Rasmussen [36]. The two lowest spin changes,  $l_\alpha$ , permitted by  $\alpha$ -decay selection rules were included in the calculations. The hindrance factors have been taken as the inverse of these reduced decay widths scaled so that  $\text{HF}(^{212}\text{Po} \rightarrow ^{208}\text{Pb}) = 1$ , where  $\delta^2(^{212}\text{Po} \rightarrow ^{208}\text{Pb}) = 71.4$  keV.

Figure 4(a) shows the  $\alpha$ -decay hindrance factors from high-spin states in the four known  $\alpha$ -decaying, odd-odd,  $N = 85$  isotones to states in the  $N = 83$  daughter nuclei. The spins, parities and configurations assigned to the de-

caying states are labelled on the top axis, with those of the populated states in the inset box of the lower panel. The hindrance factors from  $^{152}\text{Ho}$  and  $^{154}\text{Tm}$  were calculated using total  $\alpha$ -decay branching ratios of 10.8(17) %, and 58(5) % respectively [9, 37]. Due to the uncertainty of the spin for the 60-keV state populated in  $^{154}\text{Lu}$  both possible hindrance factor values are given. Figure 4(b) shows the energies of the states in  $N = 83$  nuclei populated following the  $\alpha$  decays taken relative to the  $9^+$  ground states. All values reported for the first time of either hindrance factors (a) or level energies (b) are shown as full symbols.

Of the four high-spin,  $\alpha$ -decaying states considered, three, in  $^{152}\text{Ho}$ ,  $^{154}\text{Tm}$ , and  $^{158}\text{Ta}$ , have been assigned with a  $(\pi h_{11/2}\nu f_{7/2})9^+$  configuration [18–20]. The exception in the chain is  $^{156}\text{Lu}$ , where the  $\alpha$ -decaying state has recently been assigned to a  $(\pi h_{11/2}\nu h_{9/2})10^+$  configuration [21]. By comparing the  $\alpha$ -decay hindrance factors from these four states to states which have the same configuration in each of the daughter nuclei the validity of the assignments for the initial states may be assessed.

Considering the hindrance factors to the set of  $(\pi h_{11/2}\nu f_{7/2})8^+$  states found in each of the  $N = 83$  daughter isotones there is a clear order-of-magnitude increase for the  $\alpha$  decay from  $^{156}\text{Lu}$  compared with those from  $^{152}\text{Ho}$  and  $^{158}\text{Ta}$ . As all the populated states have been assigned with the same configuration, this would indicate a difference in configuration of the decaying state in  $^{156}\text{Lu}$ . These results are therefore consistent with the  $(\pi h_{11/2}\nu h_{9/2})10^+$  configuration assignment of the  $\alpha$ -decaying state in  $^{156}\text{Lu}$  differing from the  $(\pi h_{11/2}\nu f_{7/2})9^+$  assignments in the other isotones.

Hindrance factors to the  $9^+$  ground states in  $N = 83$  daughter nuclei again show a significant difference in the value from  $^{156}\text{Lu}$  compared with those from  $^{152}\text{Ho}$ ,  $^{154}\text{Tm}$ , and  $^{158}\text{Ta}$ . However, the lower value from  $^{156}\text{Lu}$  may be considered unexpected given the change in configuration required between initial,  $(\pi h_{11/2}\nu h_{9/2})10^+$ , and final,  $(\pi h_{11/2}\nu f_{7/2})9^+$ , states compared with the other three nuclei where  $(\pi h_{11/2}\nu f_{7/2})9^+$  structures are assigned to both. One possible explanation for this is the effect of blocking caused by an odd nucleon in the parent nucleus populating an orbital at the fermi surface, effectively reducing the preformation probability of the  $\alpha$  particle [38]. This could be the reason for the increase in hindrance factors of the  $\alpha$  decays from states where the odd nucleon occupies the  $f_{7/2}$  orbital [ $^{152}\text{Ho}(9^+)$ ,  $^{154}\text{Tm}(9^+)$ ,  $^{158}\text{Ta}(9^+)$ ] compared with that where it occupies the  $h_{9/2}$  orbital [ $^{156}\text{Lu}(10^+)$ ]. It is also possible that the wave functions of the states involved are not pure single-particle configurations.

The similarities of both the hindrance factors to, and energies of, the states at 238 keV in  $^{148}\text{Tb}$  and 197 keV in  $^{150}\text{Ho}$  would suggest the same structural configurations. As the state in  $^{148}\text{Tb}$  has previously been assigned as the  $7^+$  member of the  $(\pi h_{11/2}\nu f_{7/2})$  multiplet [15, 16], this configuration will also be assumed for the 197 keV state

in  $^{150}\text{Ho}$ . The configuration of the newly identified state at 60 keV in  $^{154}\text{Lu}$  is uncertain. Possible  $J^\pi$  values of  $8^+$ ,  $9^+$ , or  $10^+$ , from the  $M1$  assignment for the 60-keV transition (see Sec. V), and a large hindrance factor to the state are both incompatible with the configuration of the  $7^+$  states in  $^{148}\text{Tb}$  and  $^{150}\text{Ho}$ .

## VII. SUMMARY

The fine structure in the  $\alpha$  decay of high-spin isomers in the  $N = 85$ , odd-odd nuclei  $^{156}\text{Lu}$  and  $^{158}\text{Ta}$  have been studied for the first time. Weak  $\alpha$ -decay branches were identified to one excited state in  $^{152}\text{Tm}$  and two in  $^{154}\text{Lu}$  following the  $\alpha$  decays of  $^{156}\text{Lu}(10^+)$  and  $^{158}\text{Ta}(9^+)$  respectively. One of the states populated in  $^{154}\text{Lu}$ , at 60 keV, had not been previously observed. The systematics of the  $\alpha$ -decay hindrance factors from high-spin isomers in all four of the known  $\alpha$ -decaying, odd-odd,  $N = 85$  isotones were reviewed. The results prove consistent with the  $(\pi h_{11/2}\nu h_{9/2})10^+$  assignment of the  $\alpha$ -decaying state in  $^{156}\text{Lu}$ , which differs from those in the other three isotones,  $^{152}\text{Ho}$ ,  $^{154}\text{Tm}$ , and  $^{158}\text{Ta}$ , which have been assigned as  $(\pi h_{11/2}\nu f_{7/2})9^+$ .

This work has been supported by the United Kingdom Science and Technology Facilities Council; the Academy of Finland under the Finnish Center of Excellence Programme (2012-2017); the EU 7<sup>th</sup> framework programme, Project No. 262010 (ENSAR); the Slovak Research and Development Agency under Contract No. APVV-15-0225; and the Slovak grant agency VEGA (contract No. 2/0129/17). The authors also thank the GAMMAPOOL European Spectroscopy Resource for the loan of the detectors of the JUROGAM II array.

TABLE I:  $\alpha$ -particle energies,  $E_\alpha$ , branching ratios,  $b_\alpha$ , reduced decay widths,  $\delta^2$ , and hindrance factors, HF, of  $\alpha$  decays from  $^{156}\text{Lu}(10^+)$  and  $^{158}\text{Ta}(9^+)$  to final states with  $J_f^\pi$  and excitation energy  $E_f$  (taken from measured  $\gamma$ -ray energies) in  $^{152}\text{Tm}$  and  $^{154}\text{Lu}$ . Total decay  $Q$  values,  $Q_T$ , are given by  $Q_\alpha + E_f$ .

$E_\alpha$ (keV)	$J_f^\pi$	$E_f$ (keV)	$Q_T$ (keV)	$b_\alpha$ (%)	$\delta^2$ (keV)	HF
$^{156}\text{Lu}(10^+)$						
5561(4)	$9^+$	0	5707(4)	98(9)	85(8)	0.83(8)
5446(5)	$8^+$	114.9(5)	5704(6)	0.056(10)	0.15(3)	470(80)
$^{158}\text{Ta}(9^+)$						
6041(4)	$9^+$	0	6198(4)	96(13)	21(3)	3.4(5)
6021(4)	$8^+$	22.2(5)	6200(4)	2.7(5)	1.6(3)	44(8)
5981(4)	$(9)^+$	59.9(5)	6197(4)	$9.9(24)\times 10^{-2}$	$3.6(9)\times 10^{-2}$	2000(500)
	$(8,10)^+$				$8.1(20)\times 10^{-2}$	870(210)

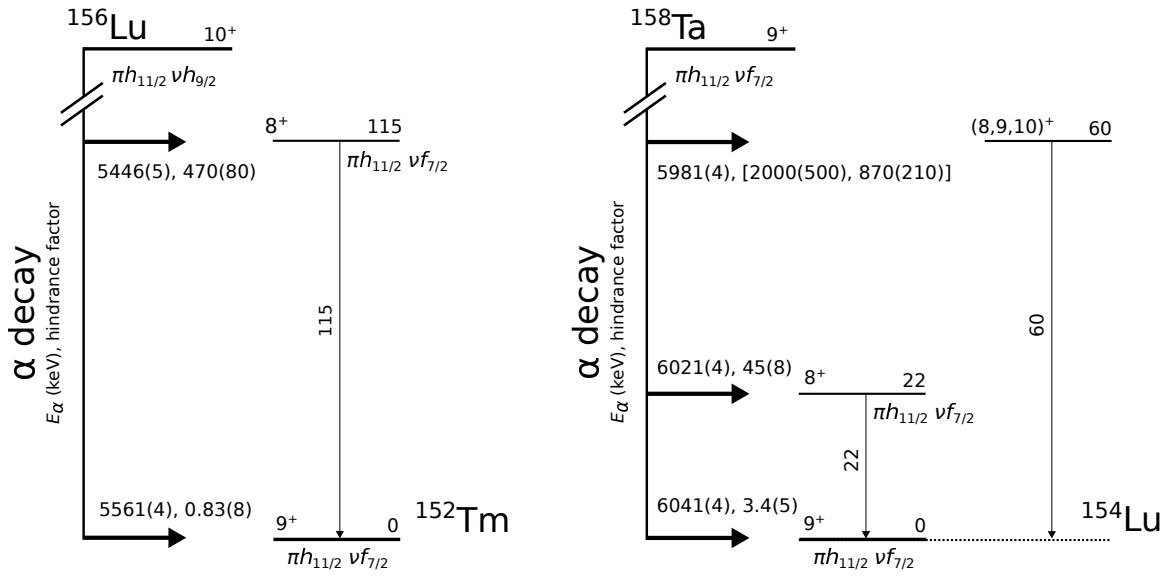


FIG. 1: Level schemes of  $^{152}\text{Tm}$  and  $^{154}\text{Lu}$  populated following the  $\alpha$  decays of  $^{156}\text{Lu}(10^+)$  and  $^{158}\text{Ta}(9^+)$ , respectively. The spins, parities and energies of each level are given along with the energies of the transitions (in keV). For each  $\alpha$  decay the  $\alpha$ -particle energies and hindrance factors are given and the state populated is also indicated. The structures which have previously been assigned to states are shown (see text for details).

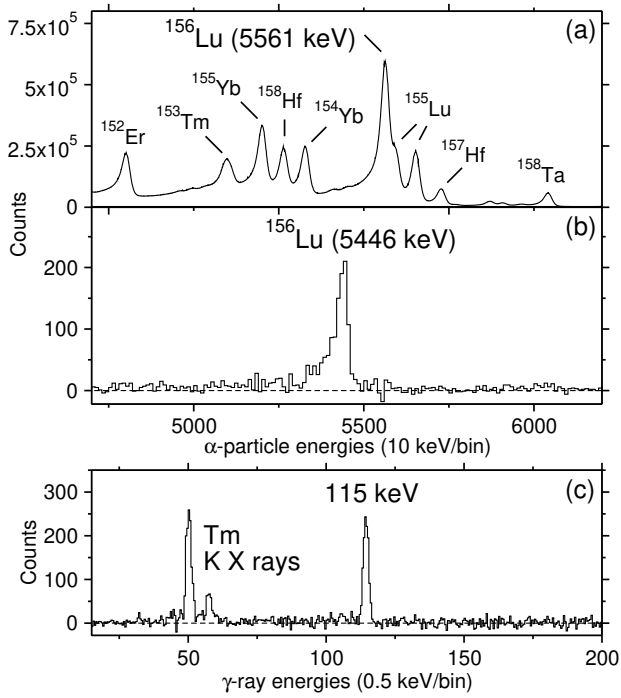


FIG. 2: Energies of  $\alpha$  particles and  $\gamma$  rays measured in the DSSD and planar germanium focal-plane detectors respectively following the decay of  $^{156}\text{Lu}(10^+)$ . Panel (a) shows the  $\alpha$ -particle energies measured up to 576 ms after a recoil implantation in the same pixel. Panel (b) shows those from (a) that are observed in coincidence with a 115-keV  $\gamma$  ray. Panel (c) shows the  $\gamma$  and K X rays measured in coincidence with the 5446-keV  $\alpha$  particles. Background subtraction has been applied to spectra in Panels (b) and (c).



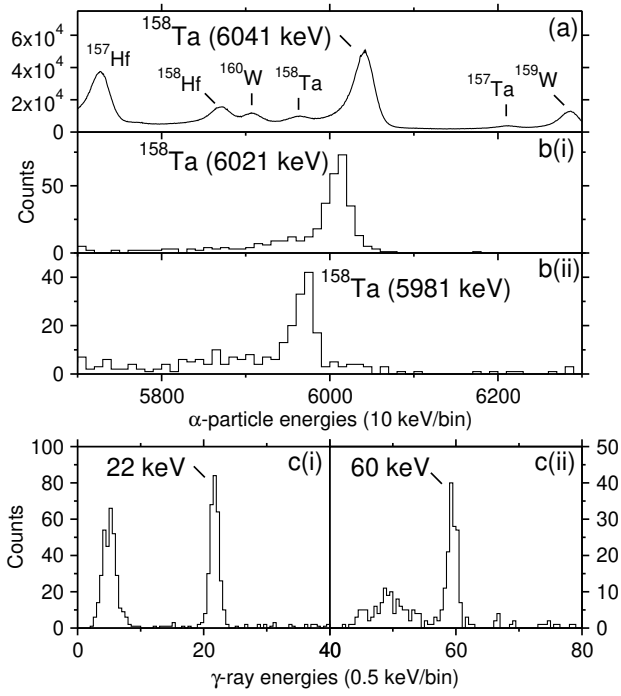


FIG. 3: Energies of  $\alpha$  particles and  $\gamma$  rays measured in the DSSD and planar germanium focal-plane detectors respectively following the decay of  $^{158}\text{Ta}(9^+)$ . Panel (a) shows the  $\alpha$ -particle energies measured up to 105 ms after a recoil implantation in the same pixel. Panels b(i) and (ii) show the same counts as (a) but with the requirement of a coincident  $\gamma$  ray with energy 22 or 60 keV, respectively. Panels c(i) and (ii), conversely, show the  $\gamma$  rays measured in coincidence with the 6021- and 5981-keV  $\alpha$  particles.

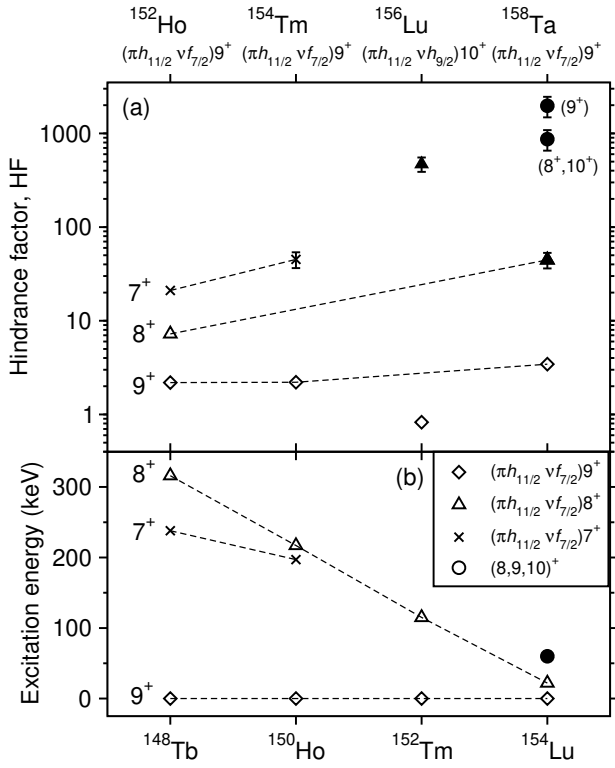


FIG. 4: (a)  $\alpha$ -decay hindrance factors from high-spin states of odd-odd,  $N = 85$  isotones to states in  $N = 83$ , daughter nuclei. The spins, parities and configurations of the decaying states are shown on the upper axis with those of the populated states indicated in the inset of the lower panel (where assignments have been made). (b) The energies of the states populated in the daughter nuclei, indicated on the lower axis, relative to the  $9^+$  ground states. Error bars which lie within the symbols have been omitted and newly measured values for either hindrance factors (a) or level energies (b) are shown as full symbols. Points that are linked by dashed lines in the lower panel are sets of final states with the same configuration and those in the upper panel which also have the same initial state in the  $\alpha$ -decay process.

- [1] M. Ogawa, R. Broda, K. Zell, P. J. Daly, and P. Kleinheinz. *Phys. Rev. Lett.*, **41**:289–292, (1978).
- [2] P. Kleinheinz, S. Lunardi, M. Ogawa, and M. R. Maier. *Z. Phys. A: At. Nucl.*, **284**(1):351–352, (1978).
- [3] P. Kleinheinz, M. Ogawa, R. Broda, P. J. Daly, D. Haenni, H. Beuscher, and A. Kleinrahm. *Z. Phys. A: At. Nucl.*, **286**(1):27–29, (1978).
- [4] I. G. Darby, R. D. Page, D. T. Joss, J. Simpson, L. Bianco, R. J. Cooper, S. Eeckhaudt, S. Ertürk, B. Gall, T. Grahn, P. T. Greenlees, B. Hadinia, P. M. Jones, D. S. Judson, R. Julin, S. Juutinen, S. Ketelhut, M. Leino, A.-P. Leppänen, M. Nyman, P. Rakhkila, J. Sarén, C. Scholey, A. N. Steer, J. Uusitalo, and M. Venhart. *Phys. Lett. B*, 695(1):78, (2011).
- [5] R. D. Macfarlane and R. D. Griffioen. *Phys. Rev.*, **130**:1491–1498, (1963).
- [6] K. S. Toth, R. L. Hahn, M. A. Ijaz, and W. M. Sample. *Phys. Rev. C*, **2**:1480–1490, (1970).
- [7] J. D. Bowman, R. E. Eppley, and E. K. Hyde. *Phys. Rev. C*, **25**:941–951, (1982).
- [8] R. D. Macfarlane. *Phys. Rev.*, **136**:B941–B947, (1964).
- [9] K. S. Toth, D. C. Sousa, J. C. Batchelder, J. M. Nitschke, and P. A. Wilmarth. *Phys. Rev. C*, **56**:3410–3413, (1997).
- [10] H. Gauvin, Y. Le Beyec, J. Livet, and J. L. Reyss. *Ann. Phys.*, **9**:241, (1975).
- [11] S. Hofmann, W. Faust, G. Münzenberg, W. Reisdorf, P. Armbruster, K. Güttner, and H. Ewald. *Z. Phys. A*, **291**(1):53–70, (1979).
- [12] R. D. Page, P. J. Woods, R. A. Cunningham, T. Davinson, N. J. Davis, A. N. James, K. Livingston, P. J. Sellin, and A. C. Shotter. *Phys. Rev. C*, **53**:660–670, (1996).
- [13] C. N. Davids, P. J. Woods, J. C. Batchelder, C. R. Bingham, D. J. Blumenthal, L. T. Brown, B. C. Busse, L. F. Conticchio, T. Davinson, S. J. Freeman, D. J. Henderson, R. J. Irvine, R. D. Page, H. T. Penttilä, D. Seweryniak, K. S. Toth, W. B. Walters, and B. E. Zimmerman. *Phys. Rev. C*, **55**:2255–2266, (1997).
- [14] R. J. Carroll, R. D. Page, D. T. Joss, J. Uusitalo, I. G. Darby, K. Andgren, B. Cederwall, S. Eeckhaudt, T. Grahn, C. Gray-Jones, P. T. Greenlees, B. Hadinia, P. M. Jones, R. Julin, S. Juutinen, M. Leino, A.-P. Leppänen, M. Nyman, D. O’Donnell, J. Pakarinen, P. Rakhkila, M. Sandzelius, J. Sarén, C. Scholey, D. Seweryniak, and J. Simpson. *Phys. Rev. Lett.*, 112:092501, 2014.
- [15] J. Styczen, P. Kleinheinz, W. Starzecki, B. Rubio, G. de Angelis, C. F. Liang, P. Paris, R. Rainhard, P. von Brentano, and J. Blomqvist. Proc. 5th int. conf. nuclei far from stability (disc. rosseau lake, canada, 1987). (1987).
- [16] C. F. Liang, P. Paris, B. Rubio, J. Styczen, and P. Kleinheinz. *JUEL-SPEZ*, **403**:31, (1987).
- [17] K. S. Toth, C. R. Bingham, H. K. Carter, B. G. Ritchie, D. C. Sousa, and D. R. Zolnowski. *Phys. Rev. C*, **20**:298–306, (1979).
- [18] S. André, C. Foin, D. Santos, D. Barnéoud, J. Genevey, Ch. Vieu, J.S. Dionisio, M. Pautrat, C. Schüch, and Z. Meliani. *Nucl. Phys. A*, **575**(1):155–174, (1994).
- [19] C. Foin, A. Gizon, J. Genevey, J. Gizon, P. Paris, F. Farget, D. Santos, D. Barnéoud, and A. Plochocki. *Eur. Phys. J. A*, **14**(1):7–11, (2002).
- [20] R. J. Carroll, B. Hadinia, C. Qi, D. T. Joss, R. D. Page, J. Uusitalo, K. Andgren, B. Cederwall, I. G. Darby, S. Eeckhaudt, T. Grahn, C. Gray-Jones, P. T. Greenlees, P. M. Jones, R. Julin, S. Juutinen, M. Leino, A.-P. Leppänen, M. Nyman, J. Pakarinen, P. Rakhkila, M. Sandzelius, J. Sarén, C. Scholey, D. Seweryniak, and J. Simpson. *Phys. Rev. C*, **94**:064311, (2016).
- [21] M. C. Lewis, E. Parr, R. D. Page, C. McPeake, D. T. Joss, F. A. Ali, K. Auranen, A. D. Briscoe, L. Capponi, T. Grahn, P. T. Greenlees, J. Henderson, A. Herzán, U. Jakobsson, R. Julin, S. Juutinen, J. Konki, M. Labiche, M. Leino, P. J. R. Mason, M. Nyman, D. O’Donnell, J. Pakarinen, P. Papadakis, J. Partanen, P. Peura, P. Rakhkila, J. P. Revill, P. Ruotsalainen, M. Sandzelius, J. Sarén, B. Saygı, C. Scholey, J. Simpson, J. F. Smith, M. Smolen, J. Sorri, S. Stolze, A. Thornthwaite, and J. Uusitalo. *Phys. Rev. C*, 98:024302, (2018).
- [22] R. Broda, M. Behar, P. Kleinheinz, P. J. Daly, and J. Blomqvist. *Z. Phys. A*, **293**(2):135–149, (1979).
- [23] C. Schumacher, P. von Brentano, A. Dewald, M. Eschenauer, H. Grawe, J. Heese, K. H. Maier, M. Philipp, E. Radermacher, R. Schubart, O. Stuch, J. Theuerkauf, D. Weißhaar, M. Wilhelm, and K. O. Zell. *Z. Phys. A*, **352**(2):161–162, (1995).
- [24] J. Wilson, Y. H. Chung, S. R. Faber, A. Pakkanen, P. J. Daly, I. Ahmad, P. Chowdhury, T. L. Khoo, R. D. Lawson, and R. K. Smither. *Phys. Lett. B*, **103**(6):413–416, (1981).
- [25] J. McNeill, R. Broda, Y. H. Chung, P. J. Daly, Z. W. Grabowski, H. Helppi, M. Kortelahti, R. V. F. Janssens, T. L. Khoo, R. D. Lawson, D. C. Radford, and J. Blomqvist. *Z. Phys. A*, **325**(1):27–35, (1986).
- [26] J. H. McNeill, J. Blomqvist, A. A. Chishti, P. J. Daly, W. Gelletly, M. A. C. Hotchkis, M. Piiparinen, B. J. Varley, and P. J. Woods. *Z. Phys. A*, **335**(2):241–242, (1990).
- [27] J. H. McNeill, A. A. Chishti, P. J. Daly, W. Gelletly, M. A. C. Hotchkis, M. Piiparinen, B. J. Varley, P. J. Woods, and J. Blomqvist. *Z. Phys. A*, **344**(4):369–379, (1993).
- [28] M. Leino. *Nucl. Instrum. Methods Phys. Res., Sect. B*, **126**(1-4):320, (1997).
- [29] J. Uusitalo, P. Jones, P. Greenlees, P. Rakhkila, M. Leino, A. N. Andreyev, P. A. Butler, T. Enqvist, K. Eskola, T. Grahn, R.-D. Herzberg, F. Heßberger, R. Julin, S. Juutinen, A. Keenan, H. Kettunen, P. Kuusiniemi, A. P. Leppänen, P. Nieminen, R. Page, J. Pakarinen, and C. Scholey. *Nucl. Instrum. Methods Phys. Res., Sect. B*, **204**:638, (2003).
- [30] R. D. Page, A. N. Andreyev, D. E. Appelbe, P. A. Butler, S. J. Freeman, P. T. Greenlees, R. D. Herzberg, D. G. Jenkins, G. D. Jones, P. Jones, D. T. Joss, R. Julin, H. Kettunen, M. Leino, P. Rakhkila, P. H. Regan, J. Simpson, J. Uusitalo, S. M. Vincent, and R. Wadsworth. *Nucl. Instrum. Methods Phys. Res., Sect. B*, **204**:634, (2003).
- [31] P. Rakhkila. *Nucl. Instrum. Methods Phys. Res., Sect. A*, **595**(3):637, (2008).
- [32] I. H. Lazarus, E. E. Appelbe, P. A. Butler, P. J. Coleman-Smith, J. R. Cresswell, S. J. Freeman, R. D. Herzberg, I. Hibbert, D. T. Joss, S. C. Letts, R. D. Page, V. F. E. Pucknell, P. H. Regan, J. Sampson, J. Simpson, J. Thorn-

- hill, and R. Wadsworth. *IEEE Trans. Nucl. Sci.*, **48**:567, (2001).
- [33] R. G. Helmer. *Nucl. Data Sheets*, 107(3):507 – 788, (2006).
- [34] H. Mahmud, C. N. Davids, P. J. Woods, T. Davinson, D. J. Henderson, R. J. Irvine, D. Seweryniak, and W. B. Walters. *Phys. Rev. C*, 62:057303, (2000).
- [35] T. Kibédi, T. W. Burrows, M. B. Trzhaskovskaya, P. M. Davidson, and C. W. Nestor Jr. *Nucl. Instrum. Methods Phys. Res. A*, **589**(2):202, (2008).
- [36] J. O. Rasmussen. *Phys. Rev.*, **113**:1593–1598, (1959).
- [37] N. Nica. *Nuclear Data Sheets*, **117**:1 – 229, (2014).
- [38] K. Van de Vel, A. N. Andreyev, M. Huyse, P. Van Duppen, J. F. C. Cocks, O. Dorvaux, P. T. Greenlees, K. Helariutta, P. Jones, R. Julin, S. Juutinen, H. Ketunen, P. Kuusiniemi, M. Leino, M. Muikku, P. Nieminen, K. Eskola, and R. Wyss. *Phys. Rev. C*, 65:064301, (2002).